XA9743314

XA9743314

International Atomic Energy Agency

INDC(CHL)-004
Distr. L0

INDC **INTERNATIONAL NUCLEAR DATA COMMITTEE**

FULL-FOLDING MODEL FOR OPTICAL POTENTIALS

H.F. Arellano and F.A. Brieva

Departamento de Física
Facultad de Ciencias Físicas y Matemáticas
Universidad de Chile
Casilla 487-3, Santiago, Chile

November 1996

IAEA NUCLEAR DATA SECTION, WAGRAMERSTRASSE 5, A-1400 VIENNA

Reproduced by the IAEA in Austria
November 1996

INDC(CHL)-004
Distr. L0

FULL-FOLDING MODEL FOR OPTICAL POTENTIALS

H.F. Arellano and F.A. Brieva

Departamento de Física
Facultad de Ciencias Físicas y Matemáticas
Universidad de Chile
Casilla 487-3, Santiago, Chile

November 1996

Full–Folding Model for Optical Potentials

H. F. Arellano and F. A. Brieva
Departamento de Física,
Facultad de Ciencias Físicas y Matemáticas,
Universidad de Chile,
Casilla 487-3, Santiago, Chile

Abstract

The development of the full folding model has set new standards for detailed microscopic calculations of nucleon–nucleus scattering. Based on realistic nucleon–nucleon interactions, this model samples the explicit off–shell behavior and the intrinsic energy dependence of the effective internucleon force in the nuclear medium as driven by the Fermi motion of the target nucleons. As a result, we have a reliable parameter–free framework to calculate with reasonable accuracy nucleon–nucleus scattering observables in the 20–500 MeV energy range. In this paper we present the foundations of the full folding model and discuss its scope and limitations. Results from calculations of differential cross sections and spin observables for proton elastic scattering from light and heavy nuclei are presented and compared to available data. The predicting power of the theory is also explored with calculations of total cross sections for neutron scattering from nuclei as a function of the projectile energy. Furthermore, we shall discuss the sensitivity of the full folding results to different choices of realistic internucleon interactions. In particular, we present recent developments based on the use of quantum inversion potentials constructed directly from nucleon–nucleon phase–shift data.

1 Introduction

It is now almost twenty years since the first microscopic optical potential calculations for elastic nucleon scattering from nuclei, starting from a realistic nucleon–nucleon (NN) interaction, were reported [1]. There, the effort was centered in determining a simplified internucleon effective force in the nuclear medium which, in turn, could be folded with the target ground state density to give a first–order description of the nucleon–nucleus (NA) optical potential. The main success of that approach was to show that a parameter–free description of the scattering process led to a fair description of the data in a reasonable range of energies, say 30 - 100 MeV. Further developments in the mid eighties extended the range of applicability of the model to incident nucleon energies of the order of 200 MeV [2, 3]. Thus, the possibility of calculating detailed optical potentials as a result of a deeper understanding of the nuclear dynamics became certain. At the same time, it diminished the role of the simpler phenomenological picture represented by the empirical models.

In recent years, new ways of approaching the NA scattering problem have provided a more complete theoretical framework for calculating the corresponding optical potentials [4, 5, 6, 7]. The efforts of several groups have been centered mainly in the 200 - 400 MeV energy range and the results obtained allow a quite accurate description of the scattering data, particularly spin observables. The essential new features introduce an explicit treatment of the off-shell behavior of the underlying NN interaction and its energy dependence as driven by the momentum distribution of nucleon in the ground state of the target nucleus. Although these new approaches were initially developed for nucleons with incident energies in the intermediate energy range, their extensions to lower incident energies have proved reasonably successful [8, 9]. Indeed, simplified nuclear matter models have been used to describe the particle propagation in the nuclear medium rather than a target-specific model, in an attempt to describe the global properties of the phenomena.

2 The Full-Folding Model

The description of the elastic scattering of a nucleon of energy E from an A-particle target relies on the reduction of the many-body Hamiltonian H_{A+1} to an effective one-body Hamiltonian $h(E)$ which correctly describes the elastic scattering channel. In the simplest formulation of the problem, let us consider an $(A+1)$-particle Hamiltonian,

$$H_{A+1} = H_A + K_0 + V \,, \tag{1}$$

where H_A is the target Hamiltonian, K_0 is the projectile kinetic energy and V is the nucleon-nucleus coupling, namely

$$V = \sum_{i=1}^{A} v_i \,, \tag{2}$$

with v_i the bare internucleon potential between the incident nucleon and the ith nucleon in the target. Then, the one-body Hamiltonian $h(E)$ for an incident nucleon of energy E becomes

$$h(E) = K_0 + U(E) \,, \tag{3}$$

and $U(E)$ is the one-body optical potential operator [10, 11, 12]. In a momentum representation, the optical potential can be expressed as

$$U(\vec{k}\,', \vec{k}\,; E) = < \vec{k}\,'; \Phi_0 | T(E + E_0) | \vec{k}\,; \Phi_0 >_{\mathcal{A}} \,, \tag{4}$$

that is, the antisymmetrized matrix elements of an $(A+1)$-body transition matrix T evaluated at the total energy $E + E_0$ in the initial state. The Φ_n are eigenstates of the A-particle target Hamiltonian H_A,

$$H_A | \Phi_n >= E_n | \Phi_n > \,, \tag{5}$$

and E_0 is the ground-state energy.

The problem of simplifying the general expression which defines the optical potential is a crucial one. It has become usual to express the many-body T-matrix in terms of a multiple-scattering series [12],

$$T(\omega) = \sum_{i=1}^{A} \left[T_i(\omega) + \sum_{j \neq i} T_i(\omega) G_{A+1}(\omega) T_j(\omega) + \ldots . \right] \,, \tag{6}$$

with $T_i(z)$ the effective interaction between the incoming particle and the ith nucleon in the target and G_{A+1} the $(A+1)$-particle propagator for the intermediate states. The leading term of this series defines the full-folding model,

$$U(\vec{k}',\vec{k};E) = \sum_{i=1}^{A} < \vec{k}';\Phi_0|T_i(E+E_0)|\vec{k};\Phi_0> \ . \tag{7}$$

The calculation of the T_i transition matrix is still prohibitive due to its many–body nature. However, it has been argued that if only two–nucleon correlations are important in the nuclear medium while other nucleons propagate without interacting with the pair, then the T_i matrix elements can be expressed in terms of the matrix elements of a two–body force F_i [6],

$$< \vec{k}'\vec{k}_1',...,\vec{k}_A'|T_i|\vec{k}\vec{k}_1,...,\vec{k}_A > \approx \delta(\vec{k}_1'-\vec{k}_1)...\delta(\vec{k}_A'-\vec{k}_A) < \vec{k}'\vec{k}_i'|F_i|\vec{k}\,\vec{k}_i > . \tag{8}$$

The effective two–body force F accounts for multiple scattering of the interacting nucleons to all orders in the ladder approximation,

$$F(\omega) = v + v\Lambda(\omega)F(\omega) \ , \tag{9}$$

with $\Lambda(\omega)$ a two–body propagator for nucleons propagating in the intermediate states [9].

The optical potential can now be casted as the convolution of an antisymmetrized two–body effective interaction with the target ground state single particle wave functions [10, 11, 12]. In momentum space reads

$$U(\vec{k}',\vec{k};E) = \int d\vec{p}\,d\vec{p}\,' \sum_{\alpha\leq\epsilon_F} \phi_\alpha^\dagger(\vec{p}\,') \left\langle \vec{k}'\vec{p}\,' \ |F(E+\epsilon_\alpha)|\,\vec{k}\,\vec{p} \right\rangle_A \ \phi_\alpha(\vec{p}) \tag{10}$$

where $\{\phi_\alpha, \epsilon_\alpha\}$ are the target ground state single–particle wave functions and corresponding energies, ϵ_F is the Fermi energy. The momenta $\vec{k}(\vec{k}')$ and $\vec{p}(\vec{p}\,')$ correspond to the initial (final) momenta of the projectile and target struck nucleon respectively. The general matrix elements of the effective interaction F are not simple to evaluate due to the lack of translational invariance for the interacting nucleons in the medium. In order to have a better insight about the behavior of these matrix elements, we have proposed to use a mixed representation for the F–matrix [9],

$$\left\langle \vec{k}'\vec{p}\,' \mid F(\omega) \mid \vec{k}\,\vec{p} \right\rangle = \frac{1}{(2\pi)^3} \int d\vec{R}\, e^{i\vec{R}\cdot(\vec{Q}-\vec{Q}')} \left\langle \vec{k}_r\,' \middle| f_{\frac{\vec{Q}+\vec{Q}'}{2}}(\omega\,;\vec{R}) \middle| \vec{k}_r \right\rangle \ . \tag{11}$$

Here we have defined the initial and final two–nucleon center-of-mass (c.m.) momenta,

$$\vec{Q} = \vec{k} + \vec{p}\,, \quad \vec{Q}' = \vec{k}' + \vec{p}\,' \ , \tag{12}$$

and the corresponding relative momenta by

$$\vec{k}_r = \tfrac{1}{2}(\vec{k}-\vec{p})\,, \quad \vec{k}_r\,' = \tfrac{1}{2}(\vec{k}'-\vec{p}\,') \ . \tag{13}$$

The function $\langle \vec{k}_r\,'|f_{\vec{Q}}(\omega\,;\,\vec{R})|\vec{k}_r\rangle$ corresponds to the matrix elements of a reduced two-body effective interaction. In the case of no dependence of the f matrix upon the spatial coordinate ($\vec{R}$) one restores total momentum conservation of the interacting pair as the radial integral in Eq. (11) leads to a c.m. momentum conserving Dirac δ-function. Using the two-body force $F(\omega)$, as expressed in Eq. (11), we obtain

$$U(\vec{k}',\vec{k};E) = \frac{1}{(2\pi)^3}\sum_{\alpha\leq\epsilon_F}\int d\vec{R}\,d\vec{P}\,d\vec{p}\,e^{i\vec{R}\cdot(\vec{q}-\vec{p})}\rho_\alpha(\vec{P}+\tfrac{1}{2}\vec{p},\vec{P}-\tfrac{1}{2}\vec{p}) \times\left\langle\vec{\kappa}'-\tfrac{1}{4}(\vec{p}-\vec{q})\,\middle|\,f_{\vec{K}+\vec{P}}(E+\epsilon_\alpha;\vec{R})\middle|\,\vec{\kappa}+\tfrac{1}{4}(\vec{p}-\vec{q})\right\rangle_{\mathcal{A}}, \tag{14}$$

where we have denoted

$$\vec{\kappa}' = \tfrac{1}{2}(\vec{K}-\vec{P}-\vec{q}), \quad \vec{\kappa} = \tfrac{1}{2}(\vec{K}-\vec{P}+\vec{q}), \tag{15}$$

with $\vec{K}$ and $\vec{q}$ defined by

$$\vec{K} = \tfrac{1}{2}(\vec{k}+\vec{k}'), \qquad \vec{q} = \vec{k}-\vec{k}', \tag{16}$$

corresponding to the average and transferred momentum of the projectile respectively; the ground state density ρ_α associated with the state α is given by

$$\rho_\alpha(\vec{P}+\tfrac{1}{2}\vec{p},\vec{P}-\tfrac{1}{2}\vec{p}) = n_\alpha\,\phi^\dagger_\alpha(\vec{P}+\tfrac{1}{2}\vec{p})\phi_\alpha(\vec{P}-\tfrac{1}{2}\vec{p}), \tag{17}$$

with n_α the occupancy of level α.

Eq. (14) represents the most general expression for the leading term of the optical potential when the effective interaction is calculated taking into account finite size effects. An advantage of this approach over now standard finite nucleus models [1, 3] is that we do not require an explicit local density assumption to convolute the effective force with the target density. Furthermore, we are able to keep track of the approximations that need to be introduced when establishing the connection between the finite many-body problem and the construction of an effective force which incorporates nuclear correlations in a realistic way.

The calculation of the optical potential as expressed by Eq. (14) is quite challenging. It involves the calculation of the reduced force f from Eq.(e9) and the evaluation of multi-dimensional integrals. In order to find a simplified expression for the optical potential, the Wigner transform [13] W_α of the single-particle density ρ_α can be introduced, namely

$$W_\alpha(\vec{R};\vec{P}) = \frac{1}{(2\pi)^3}\int d\vec{p}\,e^{-i\vec{R}\cdot\vec{p}}\,\rho_\alpha(\vec{P}+\tfrac{1}{2}\vec{p},\vec{P}-\tfrac{1}{2}\vec{p}). \tag{18}$$

Then, replacing Eq. (18) in Eq. (14) and making the change of variable $\vec{p}\to\vec{p}+\vec{q}$, we obtain

$$U(\vec{k}',\vec{k};E) = \frac{1}{(2\pi)^3}\sum_{\alpha\leq\epsilon_F}\int d\vec{R}d\vec{R}'d\vec{P}d\vec{p}\,e^{i\vec{R}'\cdot\vec{q}}W_\alpha(\vec{R}';\vec{P})\,e^{i\vec{p}\cdot(\vec{R}'-\vec{R})} \times\left\langle\vec{\kappa}'-\tfrac{1}{4}\vec{p}\,\middle|\,f_{\vec{K}+\vec{P}}(E+\epsilon_\alpha;\vec{R})\middle|\,\vec{\kappa}+\tfrac{1}{4}\vec{p}\right\rangle_{\mathcal{A}}. \tag{19}$$

Now we realize that the role of the momentum $\vec{p}$ in Eq. (19) is to give a measure of the delocalization of the average bound nucleon ($\vec{R}'$) with respect to the average incoming particle ($\vec{R}$). Since the f-matrix elements do not depend on $\vec{p}$ for an $\vec{R}$ independent interaction f, we have assumed in the general case that a weak dependence on $\vec{p}$ justifies taking $\vec{p}=0$

when evaluating the f-matrix elements in the integrand of Eq. (19). Although this approximation has not been tested, we expect it to be reasonable since the off-shell sampling is still dominated by the variation of the average momentum $\vec{P}$ of the target nucleons. Thus, the optical potential becomes

$$U(\vec{k}',\vec{k};E) \simeq \int d\vec{R}\, e^{i\vec{q}\cdot\vec{R}} \sum_{\alpha\leq\epsilon_F} \int d\vec{P}\, W_\alpha(\vec{R};\vec{P}) \left\langle \vec{\kappa}' \left| f_{\vec{K}+\vec{P}}(E+\epsilon_\alpha;\vec{R}) \right| \vec{\kappa} \right\rangle_A . \tag{20}$$

Eq. (20) is an explicit expression for the optical potential in terms of the local nuclear density in phase space (W_α) and the reduced effective force acting between the interacting nucleons at each $\vec{R}$ coordinate in the system. When the f-matrix is calculated using infinite nuclear matter correlations, then Eqs.(19) and (20) for U provide a framework for developing the local density (and other) approximations. Thus, our derivation overcomes some of the heuristic arguments often used to relate nuclear matter and finite nucleus results.

In the limit of a medium independent internucleon interaction, as in the case when using the free NN t-matrix as the effective interaction, we recover the standard expression for the full-folding optical potential [6, 14], namely $U(\vec{k}',\vec{k};E) \rightarrow U_o(\vec{k}',\vec{k};E)$, with

$$U_o(\vec{k}',\vec{k};E) = \sum_\alpha \int d\vec{P}\, \rho_\alpha(\vec{P}+\tfrac{1}{2}\vec{q},\vec{P}-\tfrac{1}{2}\vec{q}) \left\langle \vec{\kappa}' \left| t_{\vec{K}+\vec{P}}(E+\epsilon_\alpha) \right| \vec{\kappa} \right\rangle_A . \tag{21}$$

In general, the optical potential requires the calculation, at each $\vec{R}$ coordinate, of f matrices off-shell as their relative momenta obey no constraints apart from those imposed by the ground state mixed density of the target.

3 Some Results

3.1 Calculations

The results presented later in this work include several further approximations which we estimate shall not alter our findings significantly, mostly above 100 MeV incident nucleon energy.

- We take an average binding energy $\bar{\epsilon}$ for each single-particle state of the bound nucleons [14]. In this case, Eq. (20) reduces to

$$U(\vec{k}',\vec{k};E) = \int d\vec{R} \int d\vec{P}\, e^{i\vec{q}\cdot\vec{R}}\, W(\vec{R};\vec{P}) \left\langle \vec{\kappa}' \left| f_{\vec{K}+\vec{P}}(E+\bar{\epsilon};\vec{R}) \right| \vec{\kappa} \right\rangle_A , \tag{22}$$

  with $W(\vec{R};\vec{P})$ the Wigner transform of the target mixed density,

$$\begin{aligned} W(\vec{R};\vec{P}) &= \sum_\alpha W_\alpha(\vec{R};\vec{P}) \\ &= \frac{1}{(2\pi)^3} \int d\vec{p}\, e^{-i\vec{R}\cdot\vec{p}} \rho(\vec{P}+\tfrac{1}{2}\vec{p},\vec{P}-\tfrac{1}{2}\vec{p}) . \end{aligned} \tag{23}$$

- The Wigner transform is calculated using an approximated form for the mixed density [14, 15],

$$W(\vec{R};\vec{P}) = \frac{4}{(2\pi)^3}\, \rho(R)\, \frac{1}{\hat{\rho}(R)}\, \Theta[\,\hat{k}(R) - P\,] , \tag{24}$$

  with ρ the target ground state density.

- The reduced f-matrix is identified with a nuclear matter g-matrix calculated self-consistently at given values of the density [9]. This is most likely a poor approximation for nucleon scattering below 100 MeV. However, the g-matrix retains nuclear medium correlations associated with the nuclear mean field and Pauli blocking. The $\vec{R}$ dependence of the force is obtained via the relationship between the local density and a corresponding (Fermi) momentum $\hat{k}$,

$$\rho(R) \rightarrow \hat{\rho}(R) = \frac{2}{3\,\pi^3}\,\hat{k}^3(R)\,. \tag{25}$$

More realistic calculations of the effective interaction are not yet available.

- We have taken different bare NN interactions for performing optical potential calculations. They do not differ significantly in their results provided they are consistent with NN data below pion threshold. Most of the results reported here come from calculations done with the Paris potential. We have also investigated the role of newly developed NN inversion potentials [16, 17] obtained directly from NN phase–shift data in NN scattering.

3.2 Data Analysis

An interesting test for the full–folding model is the calculation of neutron total cross sections. In this case, high quality data which cover a wide range of energy and targets are available. In Fig. 1 we present calculations and data [18, 19] of total cross sections (σ_T) for neutron scattering from ^{40}Ca, ^{90}Zr and ^{208}Pb as a function of the neutron incident energy.

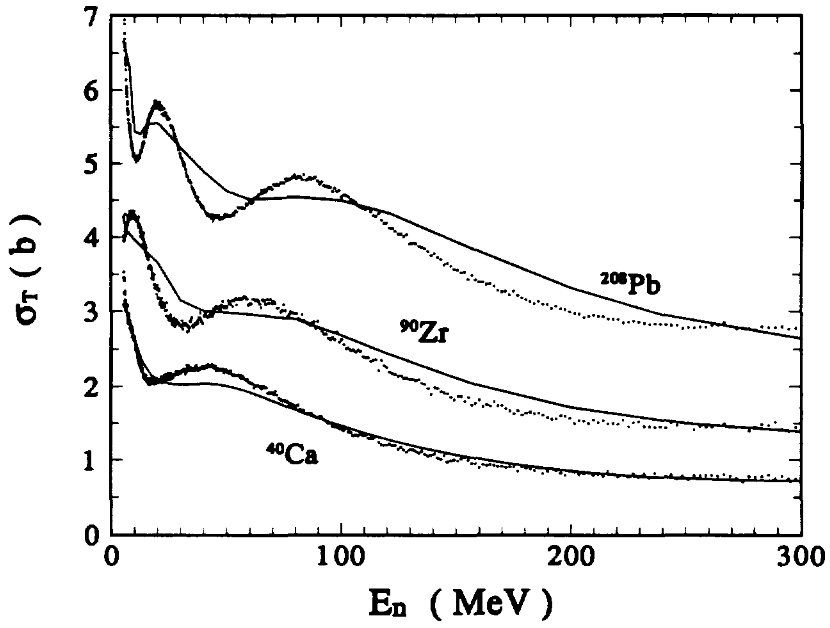

Figure 1: Measured and calculated (solid lines) total cross sections for neutron scattering from ^{40}Ca, ^{90}Zr and ^{208}Pb.

The solid curves correspond to calculations based on full–folding optical potentials with medium effects included through the g-matrix. It is worth noting that although these full–

folding calculations do not describe $\sigma_T(E)$ in detail, they do follow, on average, the energy dependence of the respective data, even at energies as low as 10 MeV. We also observe that for the heavier nuclei, particularly ^{208}Pb, the data exhibit more structure than the calculated σ_T. This feature is different from that exhibited by phenomenological calculations where the cross section is overestimated but its structure is accurately reproduced [20].

We should emphasize that the present calculations include the symmetry potential through the treatment of the folding of the effective force with the neutron and proton densities. However, the average information about the nuclear medium as provided by symmetric nuclear matter may not be sufficiently accurate to give the details of the effective force required to explain these extensive and high-precision data.

Applications have also been made for elastic scattering of protons on ^{40}Ca and ^{208}Pb. Here, calculations of differential cross sections ($d\sigma/d\Omega$) and analyzing powers (A_y) have been performed at energies between 30 and 400 MeV.

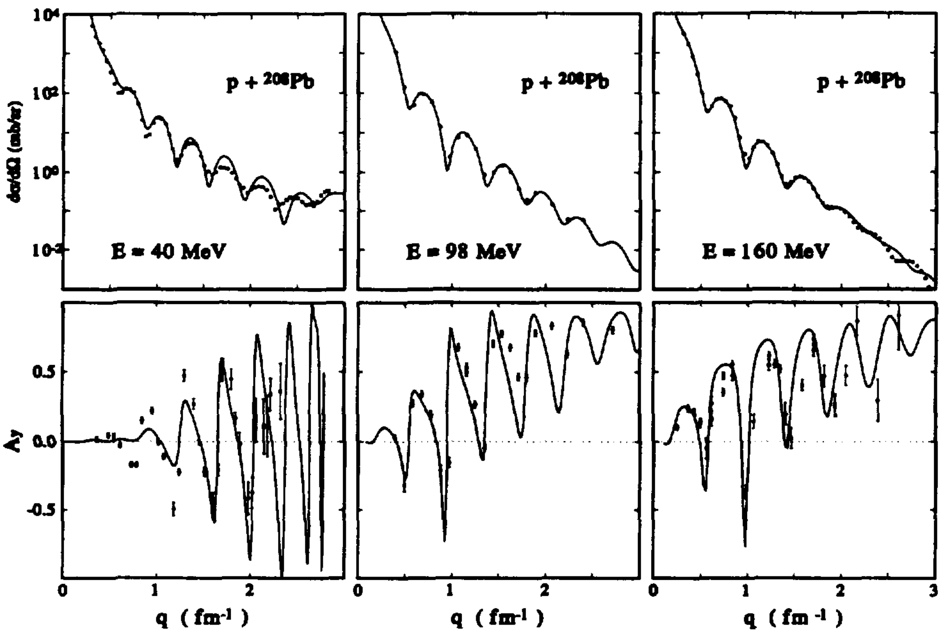

Figure 2: Measured and calculated observables for p+^{208}Pb elastic scattering at 40, 98 and 160 MeV.

In Fig. 2 we have chosen to present our results for p+^{208}Pb elastic scattering corresponding to measured observables at energies of 40 [21], 98 [22] and 160 [23] MeV. Overall, the theory improves its description of data as the energy of the proton increases. Indeed, the agreement becomes remarkable for incident proton energies of the order of 60 MeV and above [9]. Nevertheless, such a feature is not well reproduced for proton elastic scattering on lighter nuclei (^{40}Ca for example) where full-folding calculations still provide a systematic and qualitatively correct description of data but not at the level of agreement shown in the ^{208}Pb case. This result is consistent with the hypothesis used in calculating the effective

NN interaction, namely the nuclear matter g-matrix.

The full-folding model predictions for proton elastic scattering above 200 MeV will be shown for the p+^{40}Ca system. In this case, we present results obtained from the Paris potential [24] and from NN inversion potentials [17] constructed from the SM94 phase-shift analysis [25]. The main difference between the two potentials is its different on-shell behavior above pion threshold, with the Paris potential giving unconstrained and, therefore, arbitrary NN phase-shifts in that region.

In Fig. 3 we show our results for p+^{40}Ca at 200 and 300 MeV. The full line corresponds to the results from the inversion potential and the dashed curve to the results from the Paris one. The data was taken from Ref.[26] at 200 MeV and from Ref.[27] at 300 MeV. At these energies we can analyze two aspects. Firstly, the full-folding model keeps providing a detailed description of the data starting from the different bare NN forces. Secondly, we start noting some departure in the predictions of the Paris and the inversion potentials, with a tendency of the latter to be relatively closer to the NA scattering data and mainly for the spin observables. Our findings are confirmed with calculations at 400 and 500 MeV.

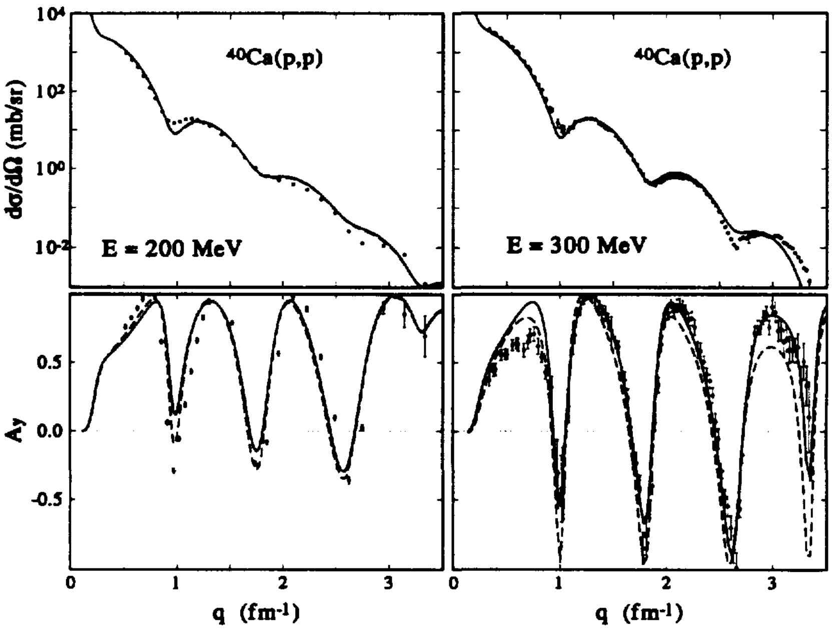

Figure 3: Calculated and measured differential cross-section and analyzing power for p+^{40}Ca elastic scattering at 200 and 300 MeV. Solid (dashed) curves correspond to results obtained with the inversion (Paris) potential.

4 Comments

We have presented the full-folding model to calculate the NA optical potential. Its main characteristic is an accurate treatment of the off-shell effects and the energy dependence of the effective NN interaction as prescribed by the Fermi motion of the nucleons in the nucleus. This approach provides a general framework for understanding, to first order, how nucleons interact in the nuclear medium.

The strong points of the model are: the wide energy range of applicability; its reasonable accuracy for reproducing systematically the data, mainly above 100 MeV and for heavier targets; its sensitivity to the off-shell effects of the underlying NN interaction and to medium effects represented by the Pauli blocking and the nuclear mean field.

Among the weak points of the model, at this stage of development, is the use of an infinite nuclear matter g-matrix as an effective interaction. This approximation needs to be improved before assessing the importance of higher order terms in the optical potential at different energies of the projectile. Also, for energies above 200 MeV, difficulties do remain in the description of spin-observables at momentum tranfers below $\sim 1\ \mathrm{fm}^{-1}$. The origin of these difficulties is not well understood.

5 Acknowledgments

F.A.B thanks Fundación Andes and the IAEA for support. Part of this research was done under FONDECYT grants 3940008 and 1960690.

References

[1] F. A. Brieva and J. R. Rook, Nucl. Phys. **A291**, 317 (1977); **A307**, 493 (1978).

[2] H. V. von Geramb, in *The Interaction Between Medium Energy Nucleons in Nuclei*, edited by H. O. Meyer (AIP, New York,1983);

[3] L. Rikus and H. V. von Geramb, Nucl. Phys. **A426**, 496 (1984).

[4] Ch. Elster, T. Cheon, E. F. Redish and P. C. Tandy, Phys. Rev. **C41**, 814 (1990).

[5] R. Crespo, R.C. Johnson and J.A. Tostevin, Phys. Rev. **C41**, 2257 (1990); **C48**, 351 (1993).

[6] H. F. Arellano, F. A. Brieva and W. G. Love, Phys. Rev. Lett. **63**, 605 (1989); Phys. Rev **C41**, 2188 (1990).

[7] L. Ray, G. W. Hoffmann and W. R. Coker, Phys. Rep. **212**, 223 (1992).

[8] C. R. Chinn, Ch. Elster, R. M. Thaler and S. P. Weppner, Phys. Rev. **C51**, 1033 (1995).

[9] H. F. Arellano, F. A. Brieva and W. G. Love, Phys. Rev. **C52**, 301 (1995).

[10] H. Feshbach, Ann. Phys. (N.Y.) **5**, 357 (1958); ibid. **19**, 287 (1962).

[11] A. K. Kerman, H. McManus and R. M. Thaler, Ann. Phys. (N.Y.) **8**, 551 (1959).

[12] A. L. Fetter and K. M. Watson, in *Advances in Theoretical Physics*, Vol. 1, edited by K.A. Brueckner (Academic Press, New York, 1965);

[13] John W. Negele and Henri Orland, in *Quantum Many-Particle Systems* (Addison-Wesley, N.Y., 1988).

[14] H. F. Arellano, W. G. Love and F. A. Brieva, Phys. Rev **C42**, 652 (1990).

[15] X. Campi and A. Bouyssy, Phys. Lett. **73B**, 263 (1978).

[16] M. Jetter and H. V. von Geramb, Phys. Rev. **C49**, 1832 (1994); M. Jetter, H. Kohlhoff and H. V. von Geramb, in *Quantum Inversion Theory and Applications*, edited by H. V. von Geramb, pp 342, (Springer–Verlag, 1994).

[17] H. F. Arellano, F. A. Brieva, M. Sander and H. V. von Geramb, Phys. Rev. **C54**, 2570 (1996).

[18] R. W. Finlay, W. P. Abfalterer, G. Fink, E. Montei, T. Adami, P. W. Lisowski, G. L. Morgan and R. C. Haight, Phys. Rev. **C47**, 237 (1993).

[19] R. W. Finlay, G. Fink, W. P. Abfalterer, P. W. Lisowski, G. L. Morgan and R. C. Haight, in *Proceedings of the International Conference on Nuclear Data for Science and Technology*, edited by S. M. Qaim (Springer–Verlag, Berlin, 1992).

[20] E. D. Cooper, S. Hama, B. C. Clark and R. L. Mercer, Phys. Rev. **C47**, 297 (1993).

[21] W. T. H. van Oers, H. Haw and N. E. Davison, Phys. Rev. **C10**, 307 (1974).

[22] P. Schwandt, H.O. Meyer, W.W. Jacobs, A.D. Bacher, S.E. Vidgor, M.D. Kaitchuck and T.R. Donoghue, Phys. Rev. **C26**, 55 (1982).

[23] A. Nadasen, P. Schwandt, P.P. Singh, W.W. Jacobs, A.D. Bacher, P.T. Debevec, M.D. Kaitchuck, and J.T. Meek, Phys. Rev. **C23**, 1023 (1981).

[24] M. Lacombe, B. Loiseau, J. M. Richard, R. Vinh Mau, J. Côté, P. Pirés and R. de Tourreil, Phys. Rev. **C21**, 861 (1980).

[25] R. A. Arndt, I. I. Strakovsky and R. L. Workman, Phys. Rev. **C50**, 2731 (1994).

[26] J. J. Kelly *et al.*, Phys. Rev. **C39**, 1222 (1989).

[27] E. J. Stephenson, J. Phys. Soc. Jpn. (Suppl.) **55**, 316 (1985).

Nuclear Data Section	e-mail, INTERNET: SERVICES@IAEAND.IAEA.OR.AT
International Atomic Energy Agency	fax: (43-1)20607
P.O. Box 100	cable: INATOM VIENNA a
A-1400 Vienna	telex: 1-12645 atom a
Austria	telephone: (43-1)2060-21710

online: TELNET or FTP: IAEAND.IAEA.OR.AT
username: IAEANDS for interactive Nuclear Data Information System
username: ANONYMOUS for FTP file transfer
username: FENDL for FTP file transfer of FENDL files
For users with web-browsers: http://www.iaea.or.at